

Supplementary Information to "Stabilizing the false vacuum: Mott skyrmions"

M. Kanász-Nagy^{1,2}, B. Dóra^{1,3}, E. A. Demler² and G. Zaránd^{1a}

¹*BME-MTA Exotic Quantum Phases Research Group,
Budapest University of Technology and Economics and MTA-BME
Condensed Matter Research Group, Budapest 1521, Hungary*

²*Department of Physics, Harvard University, Cambridge, MA 02138, U.S.A and*

³*Department of Physics, Budapest University of Technology and Economics
and MTA-BME Condensed Matter Research Group, Budapest 1521, Hungary*

^a zarand@neumann.phy.bme.hu

A. SUPPLEMENTARY NOTE 1

In this section we provide estimates of the parameters of the lattice Hamiltonian in equations (2, 3). The interaction of spin-1 bosons is determined by their s-wave scattering lengths a_0 and a_2 , with a_F denoting the scattering length in the total hyperfine spin F channel. In case of antiferromagnetic interactions, such as in ^{23}Na considered in this paper, $a_2 > a_0 > 0$ and the ground state is a nematic superfluid [1]. In a deep optical lattice, the on-site interaction is given by $U_0 = \frac{2\pi^2}{3} \frac{a_0 + 2a_2}{\lambda} (V_0/E_R)^{3/4} E_R$, with the V_0 depth of the optical lattice, and the recoil energy of the optical lattice of wavelength λ given by $E_R = \frac{\hbar^2}{2m\lambda^2}$ [2]. The hopping, measured in units of U_0 , is given by

$$\frac{J}{U_0} = \frac{3}{\pi^{5/2}} \frac{\lambda}{a_0 + 2a_2} e^{-2\sqrt{V_0/E_R}}, \quad (\text{S1})$$

and can be easily controlled in an experiment by modifying the lattice depth to reach the superfluid-Mott insulator transition [2, 3]. The magnitude of the on-site spin interactions is related to U_0 by the scattering lengths [2, 4],

$$\frac{U_2}{U_0} = \frac{a_2 - a_0}{a_0 + 2a_2}. \quad (\text{S2})$$

As a result, the interaction term U_2 is suppressed, and is approximately $U_2 \approx 0.03 U_0$ in case of ^{23}Na [3, 4].

The parameters used throughout this paper are set using the scattering length of ^{23}Na , $a_0 = 2.75 \text{ nm}$, and a wavelength $\lambda = 594 \text{ nm}$ for the optical lattice as used in the experiment in Ref. 3. In the $zJ/U_0 \approx 0.2$ regime of the phase diagram the parameters become $U_0 \approx 250 \text{ nK}$, $U_2 \approx 6 \text{ nK}$ and $zJ \approx 50 \text{ nK}$, with $z = 6$ the number of nearest neighbors. Considering 10^5 atoms in the trap, the radius of the skyrmion is approximately $R = 30 a \approx 10 \mu\text{m}$, with the lattice constant $a = \lambda/2 \approx 0.3 \mu\text{m}$.

B. SUPPLEMENTARY NOTE 2

Here we analyze the structure of the local part of the free energy, $F_{\text{loc},\mathbf{r}}$, in equations (4, 13), and discuss its numerical evaluation. Due to the $O(3)$ symmetry of the Hamiltonian in equations (2, 3), $F_{\text{loc},\mathbf{r}}$ can be written as a function of the two rotation-invariant quantities of the $F = 1$ spin sector: the superfluid density ($\varrho_{\mathbf{r}}$), and the magnetic moment ($\mathbf{f}_{\mathbf{r}} = |\mathbf{f}_{\mathbf{r}}|$). In our numerical simulations, in order to evaluate equation (13), we truncate the Hilbert

space at 5 particles per site, and carry out the trace numerically. Fig. S1 shows plots of $F_{\text{loc},\mathbf{r}}$ in case of nematic ($U_2 > 0$) and ferromagnetic ($U_2 < 0$) interactions. Nematic condensates favor zero magnetization, $\mathbf{f}_{\mathbf{r}} \equiv 0$, and thus, the structure of the nematic ground state configuration space is $(S^2 \times U(1))/\mathbb{Z}_2$. Indeed, in the angular momentum basis of spin matrices, $(F_\alpha)_{\beta\gamma} = -i\epsilon_{\alpha\beta\gamma}$, the zero magnetization condition implies $\text{Im}(\bar{\Psi}_\alpha \Psi_\beta) = 0$ for all $\alpha\beta = x, y, z$. Thus, up to a phase factor, $\Psi(\mathbf{r})$ is given by a real vector, as shown in equation (1). Ferromagnetic condensates, on the other hand, are fully magnetized $\mathbf{f}_{\mathbf{r}} \equiv 1$, and thus, their ground state configuration space is $SO(3)$ [1]. This topological structure, however, holds no topologically protected 'Mott skyrmion' configurations.

C. SUPPLEMENTARY NOTE 3

In order to get an order of magnitude estimate of the excitation energies of the skyrmion, we need to estimate the parameters of the two-dimensional effective Lagrangian in equation (7), whose structure is dictated by the $SO(3)$ symmetry of the underlying model. Therefore, in this part of the Supplementary Information, we relate these parameters to those of the lattice Hamiltonian in equations (2, 3). Note, that the accuracy of this estimation does not influence the ratio of the excitation energies of the skyrmion and of the trivial sector, shown in Fig. 3.

We approximate the superfluid shell of the skyrmion by a two-dimensional slab of thickness $N \approx 10$ lattice sites in the z direction, and we describe it with the action

$$\mathcal{S} = \int dt \sum_{\mathbf{r}\alpha} i\bar{b}_{\mathbf{r}\alpha} \partial_t b_{\mathbf{r}\alpha} - \left(H_{\text{kin}} + \sum_{\mathbf{r}} H_{\text{loc},\mathbf{r}} \right), \quad (\text{S3})$$

where the Hamiltonian has been defined in equations (2, 3). By assuming a constant, time-independent profile in the z -direction for low-energy excitations, we can approximate the action, using the two-dimensional effective Lagrangian in equation (7),

$$\mathcal{S} \approx N \int dt \int d^2r \mathcal{L}[\bar{\psi}, \psi], \quad (\text{S4})$$

where we have introduced the continuum fields ψ_α through the substitution $b_{\mathbf{r}\alpha}/a \rightarrow \psi_\alpha(\mathbf{r})$, using the lattice constant a . Thus, the parameters of the Lagrangian are given by $m = 1/(2Ja^2)$, $\tilde{\mu} = \mu + 6Jz$, $g_0 = U_0 a^2$ and $g_2 = U_2 a^2$. In the weak coupling limit $zJ \gg U_0, U_2$ this Lagrangian density can be used to describe the excitation spectrum in the saddle

point approximation, as shown in the main text. In the strongly interacting limit quantum corrections renormalize the parameters of the Lagrangian density. We assume, however, that these effects do not change the order of magnitude of excitation energies significantly, and therefore we use the bare parameters above to estimate them.

The low energy excitations are of the order $E_0 = 1/(mR\xi_2) = \sqrt{g_2\rho/mR^2}$ both in the skyrmion and in the trivial configuration. Assuming a superfluid density $\rho = 0.5/a^2$, we estimate

$$E_0 \approx \frac{\sqrt{U_2 J}}{R/a} \approx 10 \text{ Hz} \quad (\text{S5})$$

for the ^{23}Na system with the lattice parameters given in Supplementary Note 1. Given the increased stability of the 'Mott skyrmion' considered here, these frequencies should be in the measurable range.

D. SUPPLEMENTARY NOTE 4

In what follows, we determine and compare the Bogoliubov excitation spectra of the trivial and the skyrmion configurations. The excitations were analyzed using the effective Lagrange density in equation (7), considering a thin superfluid shell of radius R . Assuming spherically symmetric ground state both in the trivial ($\psi_t = \sqrt{\rho_t} \hat{\mathbf{z}}$) and in the skyrmion configuration ($\psi_s = \sqrt{\rho_s} \hat{\mathbf{r}}$), we determined the two-dimensional superfluid densities using the saddle point equation $\delta\mathcal{L}/\delta\bar{\psi} = 0$. This equation yields $\rho_t = \mu/g_0$ and $\rho_s = (\mu - 1/(mR^2))/g_0$, respectively. In the skyrmion case, the chemical potential gets renormalized due to the curvature of the ground state. This curvature effect leads to the depletion of the superfluid density and affects the excitation spectrum as well.

In the trivial configuration, phase and spin excitations associated with the fluctuations parallel ($\delta\psi_{t\parallel}$) and perpendicular ($\delta\psi_{t\perp}$) to the ground state ψ_t , decouple to leading order. The fluctuation part of the Lagrangian, expanded up to quadratic order, reads $\delta\mathcal{L} = i\delta\bar{\psi} \partial_t \delta\psi - \mathcal{H}$, with the Hamiltonian density defined as

$$\begin{aligned} \mathcal{H}_t = & \delta\bar{\psi}_t \left(-\frac{\Delta_2}{2m} \delta\psi_t \right) + g_0\rho_t \left(|\delta\psi_{t\parallel}|^2 + \frac{\delta\psi_{t\parallel}^2 + \delta\bar{\psi}_{t\parallel}^2}{2} \right) \\ & + g_2\rho_t \left(|\delta\psi_{t\perp}|^2 - \frac{\delta\psi_{t\perp}^2 + \delta\bar{\psi}_{t\perp}^2}{2} \right). \end{aligned} \quad (\text{S6})$$

The Bogoliubov excitation energies can be obtained by treating the above Hamiltonian quantum mechanically, or, equivalently, by determining the eigenvalues of the equations of motions of the fields

$$i\partial_t\delta\psi_{t\parallel} = -\frac{\Delta_2}{2m}\delta\psi_{t\parallel} + g_0\rho_t(\delta\psi_{t\parallel} + \delta\bar{\psi}_{t\parallel}), \quad (\text{S7})$$

$$i\partial_t\delta\psi_{t\perp} = -\frac{\Delta_2}{2m}\delta\psi_{t\perp} + g_2\rho_t(\delta\psi_{t\perp} - \delta\bar{\psi}_{t\perp}). \quad (\text{S8})$$

These equations can be easily solved by expanding the fluctuations in terms of spherical harmonics, yielding the eigenfrequencies

$$\omega_{\text{ph},l} = \sqrt{\left(\frac{l(l+1)}{2mR^2} + g_0\rho_t\right)^2 - (g_0\rho_t)^2}, \quad (\text{S9})$$

$$\omega_{\text{sp},l} = \sqrt{\left(\frac{l(l+1)}{2mR^2} + g_2\rho_t\right)^2 - (g_2\rho_t)^2}, \quad (\text{S10})$$

with the angular momentum quantum number $l = 0, 1, \dots$. For a spherical trap, all excitations in the spin sector have a $(2l+1) \times 2$ -fold degeneracy, whereas phase excitations are $(2l+1)$ -fold degenerate. Although for a non-spherical trap the $(2l+1)$ -fold orbital degeneracy is removed, the 2-fold degeneracy of spin modes remains, due to spin symmetry. We find three zero-energy excitations (Goldstone modes) with $l = 0$ quantum numbers, corresponding to phase fluctuations and rotations of the ground state around the x and y axes. (Rotations around the z axis leave the ground state invariant, therefore, they do not give additional zero modes.) In the limit of large trap radii compared to the superfluid and magnetic healing lengths, $\xi_0 = 1/\sqrt{m\rho g_0}$ and $\xi_2 = 1/\sqrt{m\rho g_2}$, respectively, the excitation energies become

$$\omega_{\text{ph},l} \approx \frac{1}{mR\xi_0}\sqrt{l(l+1)}, \quad (\text{S11})$$

$$\omega_{\text{sp},l} \approx \frac{1}{mR\xi_2}\sqrt{l(l+1)}. \quad (\text{S12})$$

Since the spin coupling is small, $g_2 \ll g_0$, and thus the spin healing length is much larger than that of the superfluid, $\xi_2 \gg \xi_0$, the low energy spectrum is dominated by spin excitations.

In the skyrmion case, on the other hand, the topological structure of the ground state modifies the excitation spectrum significantly. The kinetic term of the Hamiltonian in equation (S6) acquires a curvature term $\Delta_2 \rightarrow \Delta_2 + 2/R^2$ due to the non-trivial spatial structure of the ground state. Therefore, the equations of motion of spin and density fluctuations,

$\delta\psi_{s\perp}$ and $\delta\psi_{s\perp}$, respectively, do not decouple and can only be described by the combined equation

$$i\partial_t\delta\psi_s = -\left(\frac{\Delta_2}{2m} + \frac{1}{mR^2}\right)\delta\psi_s + g_0\rho_s(\delta\psi_{s\parallel} + \delta\bar{\psi}_{s\parallel}) + g_2\rho_s(\delta\psi_{s\perp} - \delta\bar{\psi}_{s\perp}). \quad (\text{S13})$$

Notice that the action of the seemingly harmless Laplacian is very non-trivial: it mixes parallel and perpendicular fluctuations ($\delta\psi_{s\parallel} \leftrightarrow \delta\psi_{s\perp}$) due to the skyrmion's geometric structure, which can also be described by introducing non-Abelian vector potentials, as shown in equation (17). The excitation energies can be most conveniently found by expanding the fields in the (orthonormal) basis of vector spherical harmonic functions [5]

$$\mathbf{Y}_{lm}(\mathbf{r}) = \hat{\mathbf{r}} Y_{lm}(\mathbf{r}), \quad (\text{S14})$$

$$\mathbf{\Psi}_{lm}(\mathbf{r}) = r \nabla Y_{lm}(\mathbf{r}) / \sqrt{l(l+1)}, \quad (\text{S15})$$

$$\mathbf{\Phi}_{lm}(\mathbf{r}) = \hat{\mathbf{r}} \times \mathbf{\Psi}_{lm}(\mathbf{r}), \quad (\text{S16})$$

that are defined using the spherical harmonics, Y_{lm} , of angular momentum quantum numbers l and m . Due to their vectorial nature, vector spherical functions form a representation of the total angular momentum operators $\vec{J} = \vec{L} + \vec{F}$ with quantum numbers $(j, m_J) = (l, m)$, where the operators \vec{J} account for simultaneous spatial (\vec{L}) and spin (\vec{F}) rotations.

As can be seen from the formulas above, the vector functions \mathbf{Y}_{lm} , defined for all $l \geq 0$, always point in the radial direction; therefore, they span the space of density fluctuations $\delta\psi_{s\parallel}$. In particular, the function $\mathbf{Y}_{00} \propto \psi_s$ corresponds to the skyrmion configuration itself, and thus, the fluctuation of the corresponding expansion coefficient describes the global phase fluctuations of the skyrmion. Perpendicular fluctuations, on the other hand, are spanned by the fields $\mathbf{\Psi}_{lm}$ and $\mathbf{\Phi}_{lm}$, which are defined for $l = 1, 2, \dots$ angular momenta.

Since the Laplacian leaves the $\mathbf{\Phi}$ -sector invariant,

$$-\Delta_2 \mathbf{\Phi}_{lm} = \frac{l(l+1)}{R^2} \mathbf{\Phi}_{lm}, \quad (\text{S17})$$

excitations in this sector decouple from the $(\mathbf{Y}, \mathbf{\Psi})$ -fluctuations, and the corresponding $(2l+1)$ -fold degenerate excitation energies can be derived analytically,

$$\omega_{\mathbf{\Phi},l} = \sqrt{\left(\frac{l(l+1)-2}{2mR^2} + g_2\rho_s\right)^2 - (g_2\rho_s)^2}. \quad (\text{S18})$$

In case of large trap radii, $R \gg \xi_0, \xi_2$, these become

$$\omega_{\Phi, l} \approx \frac{1}{mR\xi_2} \sqrt{l(l+1) - 2}. \quad (\text{S19})$$

Specifically, for $l = 1$ angular momenta, we find three zero energy modes corresponding to the rotations of the skyrmion around the x , y and z axes in parameter space. Therefore, together with the global phase fluctuations in the \mathbf{Y}_{00} subspace, there are *four* Goldstone modes in the skyrmion sector. The increased number of Goldstone modes, as compared to the trivial sector, is due to the topological winding of the skyrmion.

The excitation energies of the $(\mathbf{Y}, \mathbf{\Psi})$ -sector are more complicated, since the Laplacian is non-diagonal in these fields,

$$-\Delta_2 \begin{pmatrix} \mathbf{Y}_{lm} \\ \mathbf{\Psi}_{lm} \end{pmatrix} = \frac{1}{R^2} \begin{pmatrix} l(l+1) + 2 & -2\sqrt{l(l+1)} \\ -2\sqrt{l(l+1)} & l(l+1) \end{pmatrix} \begin{pmatrix} \mathbf{Y}_{lm} \\ \mathbf{\Psi}_{lm} \end{pmatrix}, \quad (\text{S20})$$

thereby mixing parallel and perpendicular fluctuations. The excitation energies are given by the eigenvalues of the Bogoliubov-Hamiltonian

$$H_l^{\mathbf{Y}\mathbf{\Psi}} = \frac{1}{2mR^2} \begin{pmatrix} \mathbf{\Omega}_l & \mathbf{\Lambda}_m \\ -\mathbf{\Lambda}_m & -\mathbf{\Omega}_l \end{pmatrix}, \quad (\text{S21})$$

defined using the matrices

$$\mathbf{\Omega}_l = \begin{pmatrix} l(l+1) + \sqrt{2}R/\xi_0 & -2\sqrt{l(l+1)} \\ -2\sqrt{l(l+1)} & l(l+1) - 2 + \sqrt{2}R/\xi_2 \end{pmatrix} \quad (\text{S22})$$

and

$$\mathbf{\Lambda}_m = (-1)^m \sqrt{2}R \begin{pmatrix} 1/\xi_0 & 0 \\ 0 & -1/\xi_2 \end{pmatrix}. \quad (\text{S23})$$

In a spherically symmetric trap there are two branches of excitation energies for all $l = 1, 2, \dots$ angular momenta, both being $(2l+1)$ degenerate. In the $g_2 \ll g_0$ limit the lower of these branches approaches the energies of the corresponding $\omega_{\Phi, l} \sim 1/(mR\xi_2)$ spin excitations, whereas the other branch, describing mainly phase excitations, stays at large energies $\sim 1/(mR\xi_0)$.

An investigation of the $l = 1$ excitations reveals a weak instability of the spherically symmetric ground state ψ_s towards a slight uniaxial deformation, as we verified through detailed numerical simulations. This spontaneous symmetry breaking does not influence

the number of Goldstone modes, protected by symmetry, however, as indicated in Fig. 3, it slightly splits the non-zero energy excitations due the $O(3) \rightarrow O(2)$ rotational symmetry breaking of the ground state. In particular, the lower branch of the $l = 1$ excitations in the $(\mathbf{Y}, \mathbf{\Psi})$ -sector splits in a $3 \rightarrow (2 + 1)$ -manner and their energies become extremely close to zero. No such instability has been observed in our three-dimensional lattice simulations, though their real space resolution have most likely been insufficient to detect this small symmetry breaking.

E. SUPPLEMENTARY NOTE 5

In this section, we analyze the low energy absorption spectrum of the skyrmion in a lattice modulation experiment, in which atom tunneling along one axis is modulated by periodically varying the depth of the optical lattice. Specifically, modulations along the z axis correspond to a variation of the z -hopping parameter in equation (2). In terms of the two-dimensional effective model of excitations in equation (7), this corresponds to a ∂_z^2 perturbation operator, as can be seen from the discussion below equation (S4). This term has spin $F = 0$, and it is a linear combination of the tensor operators

$$T_{0,0} = (\partial_x^2 + \partial_y^2 + \partial_z^2)/\sqrt{3}, \quad (\text{S24})$$

$$T_{2,0} = (\partial_x^2 + \partial_y^2 - 2\partial_z^2)/\sqrt{6}, \quad (\text{S25})$$

with angular momentum quantum numbers $(l, m) = (0, 0)$ and $(2, 0)$, respectively.

The symmetries of our probe operators lead to selection rules for the states that can be excited in the spherically symmetric skyrmion configuration, $\psi \propto \mathbf{Y}_{00} \propto \hat{\mathbf{r}}$ [6]. Since $T_{0,0}$ and $T_{2,0}$ are derivative operators, they commute with the angular momentum $L^2 = -\Delta_2$, and they will not mix the subspace $(\mathbf{Y}_{lm}, \mathbf{\Psi}_{lm})$ vector spherical harmonics with $\mathbf{\Phi}_{lm}$ functions, the latter forming an eigenspace of L^2 (see equation (S17)). Further selection rules follow from the rotational symmetries of the perturbation operators under spatial and spin rotations, due to the Wigner-Eckart theorem [7]. Working in the basis of total angular momentum quantum numbers, it can be easily shown that the only non-vanishing matrix elements

describing excitations of the spherically symmetric skyrmion ground state are

$$\langle \mathbf{Y}_{2,0} | T_{2,0} | \mathbf{Y}_{0,0} \rangle = -\sqrt{\frac{2}{15}}, \quad (\text{S26})$$

$$\langle \Psi_{2,0} | T_{2,0} | \mathbf{Y}_{0,0} \rangle = \frac{1}{\sqrt{5}}, \quad (\text{S27})$$

$$\langle \mathbf{Y}_{0,0} | T_{0,0} | \mathbf{Y}_{0,0} \rangle = -\frac{2}{\sqrt{3}}. \quad (\text{S28})$$

Therefore, modulations of the atom tunneling along the z axis can only create $(l, m) = (2, 0)$ excitations, and only in the (\mathbf{Y}, Ψ) sector. These correspond to a high energy density excitation, and a small energy spin excitation, the latter being shown in the lower branch of the $l = 2$ levels in Fig. 3. Such low energy levels cannot be excited in the trivial configuration, whose lattice modulation spectrum contains only high energy density fluctuations, to linear order. Thus, the presence of such a low energy excitation peak in the modulation spectrum is an unambiguous fingerprint of the skyrmion texture.

-
- [1] Ho T.-L. Spinor Bose Condensates in Optical Traps. *Phys. Rev. Lett.* **81**, 742-745 (1998).
 - [2] Demler, E. & Zhou, F. Spinor Bosonic Atoms in Optical Lattices: Symmetry Breaking and Fractionalization. *Phys. Rev. Lett.* **88**, 163001 (2002).
 - [3] Xu, K. *et al.*, Sodium Bose-Einstein condensates in an optical lattice. *Phys. Rev. A* **72**, 043604 (2005).
 - [4] Stenger, J., Inouye, S., Stamper-Kurn, D. M., Miesner, H.-J., Chikkatur, A. P. & Ketterle, W. Spin domains in ground-state Bose-Einstein condensates. *Nature* **396**, 345-348 (1998).
 - [5] Hill, E. L. The theory of Vector Spherical Harmonics. *Am. J. Phys.* **22**, 211-214 (1954).
 - [6] Spontaneous symmetry breaking amounts to only $\sim 1\%$ distortion of the skyrmion, in the parameter range of ^{23}Na experiments. Thus, its effect on the excitation spectrum will be negligible, and we will assume the skyrmion to be spherically symmetric in the following discussion.
 - [7] Sakurai, J. J. *Modern Quantum Mechanics* (Addison-Wesley, 1994).

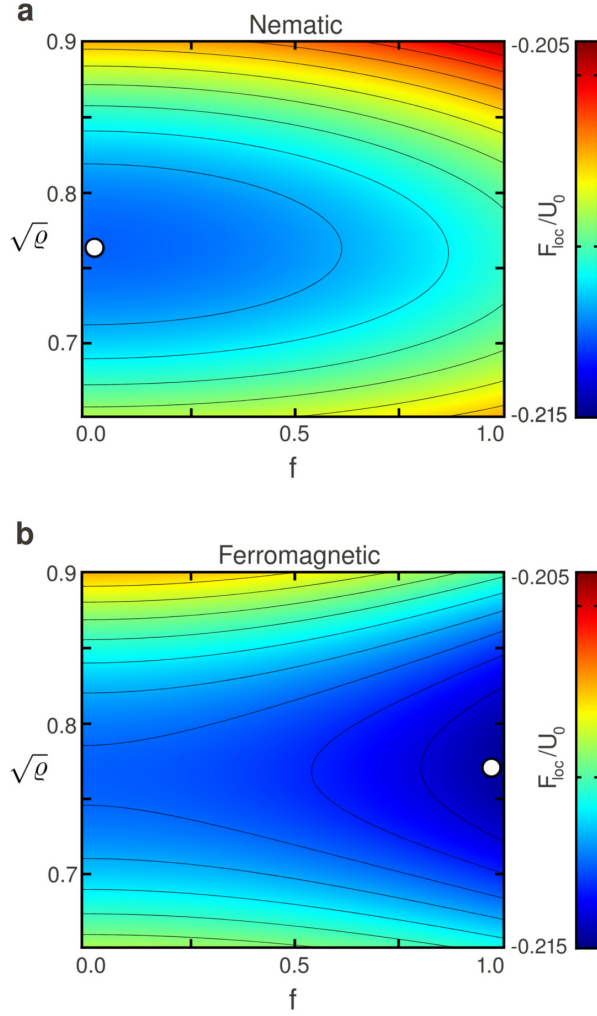


FIG. S1. **Local part of the free energy.** (a) and (b) show $F_{\text{loc}}(\varrho, f)$ in case of nematic ($U_2 > 0$) and ferromagnetic ($U_2 < 0$) interactions, respectively. The dots indicate the minima of the free energy, favoring a non-magnetized (fully magnetized) superfluid in the nematic (ferromagnetic) case. [Physical parameters of the plot: $T/U_0 = 0.05$, $U_2/U_0 = 0.025$, $zJ/U_0 = 0.40$, $\mu/U_0 = 0.08$.]